

Third- and Higher-Order Intensity Correlation in Laser Light*

C. D. Cantrell†

*Department of Physics, Swarthmore College, Swarthmore, Pennsylvania 19081
and Department of Physics, Princeton University, Princeton, N. J. 08540*

and

M. Lax

*Bell Telephone Laboratories, Murray Hill, New Jersey 07974
and City College of the City University of New York, New York, New York 10031*

and

Wallace Arden Smith

*Department of Physics, New York University, University Heights, Bronx, New York 10453
(Received 24 May 1972)*

We have calculated the third- and higher-order (multitime) cumulants of the intensity of single-mode laser light using the rotating-wave van der Pol (RWVP) model. Our results indicate a distinctly nonexponential time dependence of the cumulants slightly below threshold and an oscillatory time dependence somewhat above threshold. One can interpret this oscillatory behavior as showing that the larger fluctuations above the mean decay more rapidly than those below the mean. Measurements of the third-order intensity cumulants above threshold would be desirable to check for this behavior and to provide a more rigorous test of the RWVP model than the second-order intensity correlation.

I. INTRODUCTION

The statistics of single-mode laser light in the threshold region have been the subject of considerable experimental and theoretical study. The steady-state statistics are found to be well described by essentially the simplest physically reasonable model, the rotating-wave van der Pol (RWVP) model. However the time-dependent statistical behavior of a laser, as it relaxes towards equilibrium from a fluctuation, involves considerably more details of its dynamics than does the time-independent steady-state behavior. Experimentally, the relaxation processes are revealed in the time dependence of the multitime correlations of the intensity such as $\langle I(t_1)I(t_2) \rangle$ and $\langle I(t_1) \times I(t_2)I(t_3) \rangle$. In this paper we shall calculate the third- and higher-order intensity correlations,¹ which are more sensitive to the higher decay rates of the laser than the well-studied second-order intensity correlation. This will provide a more detailed understanding and test of the RWVP model.

A triple-photoelectron-coincidence experiment has been performed by Davidson and Mandel² on a He:Ne laser at and below threshold. These measurements are consistent with a simple exponential time decay, with a third-order coherence time which (below threshold) is distinctly shorter than the second-order intensity correlation time. According to our calculations the decay slightly below threshold departs significantly from simple exponential behavior, and the times characteristic of this decay are longer than those found by David-

son and Mandel. Above threshold, the decay becomes oscillatory. Haake³ has predicted a damped-oscillation time dependence for the intensity correlation functions of lasers where atomic "memory" effects invalidate the Markoffian assumption of the RWVP model. However, we find damped oscillatory behavior even in the RWVP model; that is, on the 10- μ sec time scale, rather than on the nanosecond time scale needed to observe non-Markoffian effects.

The additional complexity of an oscillatory correlation means that the experimental results are sensitive to some of the higher eigenvalues (decay rates) of the Fokker-Planck operator in the RWVP model. Thus, in contrast to the second-order intensity correlation, it is not possible to describe the expected third-order correlation results in terms of a single correlation time. More precise measurements would be desirable.

II. CALCULATION

It is convenient to express both experimental and theoretical results for N th-order intensity correlations in terms of quantities which contain only the true N th-order correlation, with all lower-order effects subtracted away. The quantities which fulfill this criterion are the cumulants⁴

$$K_{11}(I_1, I_2) = \langle T_N(\Delta I_1 \Delta I_2) \rangle,$$

$$K_{111}(I_1, I_2, I_3) = \langle T_N(\Delta I_1 \Delta I_2 \Delta I_3) \rangle,$$

$$K_{1111}(I_1, I_2, I_3, I_4) = \langle T_N(\Delta I_1 \Delta I_2 \Delta I_3 \Delta I_4) \rangle \\ - \langle T_N(\Delta I_1 \Delta I_2) \rangle \langle T_N(\Delta I_3 \Delta I_4) \rangle$$

$$\begin{aligned} & -\langle T_N(\Delta I_1 \Delta I_3) \rangle \langle T_N(\Delta I_2 \Delta I_4) \rangle \\ & -\langle T_N(\Delta I_1 \Delta I_4) \rangle \langle T_N(\Delta I_2 \Delta I_3) \rangle, \end{aligned} \quad (1)$$

where

$$\Delta I_j = b_j^\dagger b_j - \langle b_j^\dagger b_j \rangle;$$

$b_j = b(t_j)$ is the positive-frequency (destruction) part of the field operator at time t_j ; and T_N places the operators in normal order (creation operators to the left) and in the apex time sequence (e.g., $b_1^\dagger b_2^\dagger b_3^\dagger b_3 b_2 b_1$). Experimental results for the intensity cumulants are proportional to the average intensity, solid angles, and other efficiency factors. These can be eliminated by comparing experiment with theory for the dimensionless ratios

$$\begin{aligned} K_n(t_1, \dots, t_{n-1}) &= \langle I \rangle^{-n} K_{11\dots 1}(I(t_1 + t_2 + \dots + t_{n-1}), \\ & I(t_1 + t_2 + \dots + t_{n-2}), \dots, I(t_1), I(0)), \end{aligned} \quad (2)$$

where t_1 is the time delay between the first and second measurements of the intensity, t_2 the delay between the second and third, and so on.

The multitime correspondence between quantum and classical stochastic systems,^{5,6}

$$b(t) \rightarrow \beta(t), \quad b^\dagger(t) \rightarrow \beta^*(t),$$

is such that apex-ordered operators, as in (1), can be averaged by taking the associated c -number average:

$$\langle T_N(\Delta I_1 \Delta I_2 \Delta I_3) \rangle = \langle \Delta \rho_3 \Delta \rho_2 \Delta \rho_1 \rangle_c, \quad (3)$$

where

$$\rho_j = \rho(t_j) = |\beta(t_j)|^2 \quad (4)$$

is the intensity and

$$\Delta \rho_j = \rho_j - \langle \rho_j \rangle_c = \rho_j - \bar{\rho} \quad (5)$$

is the intensity fluctuation. The mean intensity can be denoted simply $\bar{\rho}$, since it is independent of the time t_j . Hereafter all averages will be c -number averages, and the subscript will be omitted.

The result, Eq. (3), is valid whether or not the quantum field statistics are Markoffian.⁷ Under the Markoffian assumption (and, in particular, for the RWVP model) the multitime probability density needed to carry out the indicated average in (3) factors^{5,8} so that

$$\begin{aligned} \langle \Delta \rho_3 \Delta \rho_2 \Delta \rho_1 \rangle &= \int_0^\infty d\rho_3 d\rho_2 d\rho_1 (\rho_3 - \bar{\rho}) P(\rho_3, t_3 | \rho_2, t_2) \\ &\quad \times (\rho_2 - \bar{\rho}) P(\rho_2, t_2 | \rho_1, t_1) (\rho_1 - \bar{\rho}) P_0(\rho_1), \end{aligned} \quad (6)$$

where $P_0(\rho)$ is the steady-state intensity probability distribution, and $P(\rho, t | \rho_0, t_0)$ is the conditional probability that the intensity will be ρ at time t , given that it was ρ_0 at t_0 . In general, the intensity probability distributions obey an equation of motion

$$\frac{\partial P}{\partial t} = -LP, \quad (7)$$

where L is a general linear operator. In the Fokker-Planck (or diffusion) approximation, where L is a non-Hermitian second-order differential operator, the conditional probability [or Green's-function solution of (7)] can be written in the form⁹

$$P(\rho, t | \rho_0, t_0) = \sum_{n=0}^{\infty} e^{-\Lambda_n(t-t_0)} P_n(\rho) \phi_n(\rho_0)^*, \quad (8)$$

where P_n and ϕ_n are the eigenfunctions of L and its Hermitian adjoint L^\dagger :

$$LP_n(\rho) = \Lambda_n P_n(\rho), \quad L^\dagger \phi_n(\rho) = \Lambda_n^* \phi_n(\rho). \quad (9)$$

It has been shown^{8,10} that when time reversal in the form of detailed balance is obeyed, we have

$$\phi_n(\rho)^* = P_n(\rho) / P_0(\rho), \quad (10)$$

where $P_0(\rho)$ satisfies the equation

$$LP_0(\rho) = 0, \quad (11)$$

corresponding to the eigenvalue $\Lambda_0 = 0$. While L is not in general a Hermitian operator it is equivalent to one under a similarity transform given by multiplication by $[P_0(\rho)]^{1/2}$. Thus the eigenvalues of L are real: $\Lambda_n = \Lambda_n^*$. In the RWVP model, $P_n(\rho)$ can be chosen to be real.

The triple-intensity cumulant, Eq. (6), reduces to

$$\begin{aligned} & \langle \Delta \rho(t+t_2) \Delta \rho(t) \Delta \rho(t-t_1) \rangle \\ &= \sum_{m,n=0}^{\infty} (\Delta \rho)_{0m} e^{-\Lambda_m t_2} (\Delta \rho)_{mn} e^{-\Lambda_n t_1} (\Delta \rho)_{n0} \\ &= \sum_{m,n=0}^{\infty} (\rho_{0m} - \bar{\rho} \delta_{0m}) e^{-\Lambda_m t_2} (\rho_{mn} - \bar{\rho} \delta_{mn}) \\ &\quad \times e^{-\Lambda_n t_1} (\rho_{n0} - \bar{\rho} \delta_{n0}) \end{aligned} \quad (12a)$$

$$= \sum_{m,n=1}^{\infty} e^{-\Lambda_m t_1 - \Lambda_n t_2} \rho_{m0} \rho_{n0} (\rho_{mn} - \delta_{mn} \bar{\rho}), \quad (12b)$$

where

$$(\rho^k)_{mn} = \int_0^\infty \phi_m(\rho)^* \rho^k P_n(\rho) d\rho, \quad (13a)$$

$$(\Delta \rho^k)_{mn} = \int_0^\infty \phi_m(\rho)^* (\rho - \bar{\rho})^k P_n(\rho) d\rho \quad (13b)$$

are the matrix element of the k th powers of the intensity and intensity fluctuation between the eigenfunctions of L and L^\dagger . If $k=1$ the superscript is omitted, as in (12). The mean intensity is

$$\bar{\rho} = \langle \rho \rangle = \rho_{00}. \quad (14)$$

The double-intensity cumulant can be expressed similarly as

$$\begin{aligned} \langle \Delta \rho(t) \Delta \rho(0) \rangle &= \sum_{n=0}^{\infty} (\rho_{0n} - \bar{\rho} \delta_{0n}) e^{-\Lambda_n t} \\ &\quad \times (\rho_{n0} - \bar{\rho} \delta_{n0}) \end{aligned} \quad (15a)$$

$$= \sum_{n=1}^{\infty} (\Delta\rho_{n0})^2 e^{-\Lambda_n t} . \quad (15b)$$

Note that using $\Delta\rho$ instead of ρ results in the elimination of the $n=0$ term in (15b). The normalized intensity moments about the mean are

$$H_2(t) = \langle \Delta\rho(t) \Delta\rho(0) \rangle / \bar{\rho}^2 , \quad (16a)$$

$$H_3(t_1, t_2) = \langle \Delta\rho(t_1 + t_2) \Delta\rho(t_1) \Delta\rho(0) \rangle / \bar{\rho}^3 , \quad (16b)$$

$$H_4(t_1, t_2, t_3) = \langle \Delta\rho(t_1 + t_2 + t_3) \Delta\rho(t_1 + t_2) \times \Delta\rho(t_1) \Delta\rho(0) \rangle / \bar{\rho}^4 . \quad (16c)$$

The associated normalized *cumulants* are

$$K_2(t) = H_2(t) , \quad (17a)$$

$$K_3(t_1, t_2) = H_3(t_1, t_2) , \quad (17b)$$

$$K_4(t_1, t_2, t_3) = H_4(t_1, t_2, t_3) - H_2(t_1)H_2(t_3) - H_2(t_2)H_2(t_1 + t_2 + t_3) - H_2(t_1 + t_2)H_2(t_2 + t_3) . \quad (17c)$$

When all delay times except one are zero, we have

$$K_3(t, 0) = (\bar{\rho})^{-3} \sum_{n=1}^{\infty} (\Delta\rho^2)_{0n} e^{-\Lambda_n t} (\Delta\rho)_{n0} , \quad (18a)$$

$$K_4(t, 0, 0) = (\bar{\rho})^{-4} \sum_{n=1}^{\infty} \times [(\Delta\rho^3)_{0n} - 3(\Delta\rho^2)_{00} \Delta\rho_{0n}] e^{-\Lambda_n t} (\Delta\rho)_{n0} , \quad (18b)$$

$$K_5(t, 0, 0, 0) = (\bar{\rho})^{-5} \sum_{n=1}^{\infty} \times [(\Delta\rho^4)_{0n} - 4(\Delta\rho^3)_{00} \Delta\rho_{0n} - 6(\Delta\rho^2)_{00} (\Delta\rho^2)_{0n}] \times e^{-\Lambda_n t} (\Delta\rho)_{n0} . \quad (18c)$$

III. RESULTS

To evaluate Eqs. (16) we need the eigenvalues and eigenfunctions of the Fokker-Planck operator

L. For the RWVP model,

$$-L = \frac{\partial}{\partial\rho} (2\rho^2 - 2p\rho - 4) + \frac{\partial^2}{\partial\rho^2} (4\rho) , \quad (19)$$

where p is the dimensionless net pump rate (equal to zero at threshold, positive above threshold, and negative below). Some of the numerical techniques for integrating (7) and (19) and calculating ρ_{mn} have been described elsewhere.^{11,12} The first ten nonzero eigenvalues Λ_m for assorted integral values of p in the range $-10 \leq p \leq 10$ have been published,¹² together with values of the coefficients

$$p_{0n} = (\rho_{0n})^2 / \sum_{j=1}^{\infty} (\rho_{0j})^2 . \quad (20)$$

The values of ρ_{mn} for this range of p , and values of Λ_m and $(\rho^k)_{mn}$ for $1 \leq k \leq 4$, $0 \leq m$, $n \leq 20$, are available.^{10,13}

Our numerical results for the time dependence of $H_3 = K_3$ at $p = 3, 2, 1, 0, -1$ are displayed in Figs. 1-5. Our results for $p = -2$ and -4 are not displayed. In these graphs we have measured time in units of the second-order coherence time T_c at the given intensity

$$s = t_1 \bar{\Lambda} , \quad s' = t_2 \bar{\Lambda} , \quad (21)$$

where

$$T_c \equiv (\bar{\Lambda})^{-1} = \sum_{n=1}^{\infty} p_{0n} (\Lambda_n)^{-1} . \quad (22)$$

Evidently, below threshold,

$$H(s, s') \equiv H_3(s, s') \quad (23)$$

is positive for all (normalized) times s, s' , but somewhat above threshold H_3 becomes negative for nonzero times. The third-order cumulant is a measure of the asymmetry of a probability distribution; for example, if

$$K_3(s, 0) = H_3(s, 0) = \langle \Delta\rho(s) [\Delta\rho(0)]^2 \rangle \quad (24)$$

TABLE I. Parameters to be used in the approximate expression, Eq. (25), for the third-order intensity cumulant $H_3(s, s')$.

p	$\bar{\Lambda}$	λ_1	λ_2	c_1	c_2	c_{12}	$\Delta H 10^3$	$10^2 (\Delta H / H_{\max})$
-10	21.4794	21.4694	45.0143	1.693 895 2	0.003 244 5	0.053 933 8	0.0055	0.0003
-8	17.7829	17.7667	37.9667	1.575 151 7	0.005 902 4	0.071 072 4	0.014	0.0008
-6	14.2229	14.1955	31.2890	1.387 539 4	0.011 177 8	0.094 029 4	0.041	0.0026
-4	10.8965	10.8474	25.1834	1.089 140 5	0.021 113 6	0.120 420 9	0.13	0.010
-3	9.3735	9.3070	22.4388	0.885 635 8	0.028 060 8	0.131 322 9	0.24	0.020
-2	7.9889	7.8987	19.9689	0.647 763 1	0.035 255 1	0.136 429 3	0.43	0.043
-1	6.7927	6.6721	17.8441	0.393 596 2	0.040 126 3	0.131 499 1	0.69	0.10
0	5.8539	5.7027	16.1628	0.162 067 3	0.038 637 0	0.114 249 7	1.1	0.26
1	5.2688	5.1770	15.0958	0.000 031 3	0.025 227 5	0.090 482 4	1.5	0.73
2	5.1750	3.3616	14.5447	-0.032 533 3	0.049 024 9	0.027 051 3	1.1	1.6
3	5.7508	4.4155	15.6461	-0.044 260 4	0.017 470 4	0.021 362 6	0.43	2.7
4	7.1122	5.2632	18.1747	-0.025 803 9	0.007 706 5	0.010 182 8	0.22	2.9

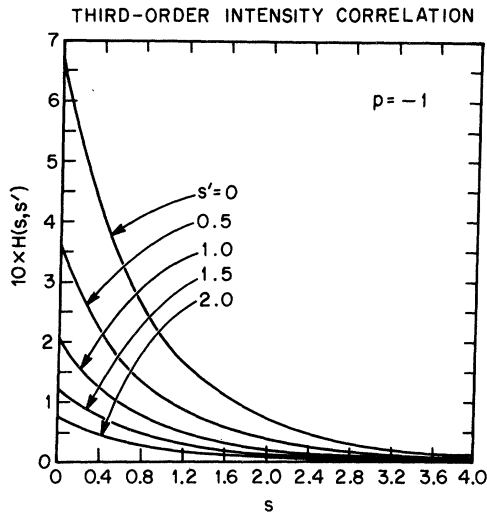


FIG. 1. Normalized third-order intensity cumulant $H(s, s')$ [Eq. (18a)] is shown as a function of the normalized time delays s and s' for pump parameter $p = -1$. The times s and s' are measured in units of the laser second-order coherence time [Eqs. (21) and (22)], and $H(s, s')$ is measured in units of $\bar{\rho}^3$, where $\bar{\rho}$ is the mean intensity at this pump parameter.

is positive, then the joint probability distribution of $\Delta\rho(s)$ and $[\Delta\rho(0)]^2$ is asymmetric towards positive fluctuations,

$$\Delta\rho(s) = \rho(s) - \bar{\rho} > 0.$$

If $K_3(s, 0) < 0$, then the distribution is asymmetric towards negative fluctuations.

Figure 6 shows that somewhat above threshold the asymmetry of the joint probability distribution

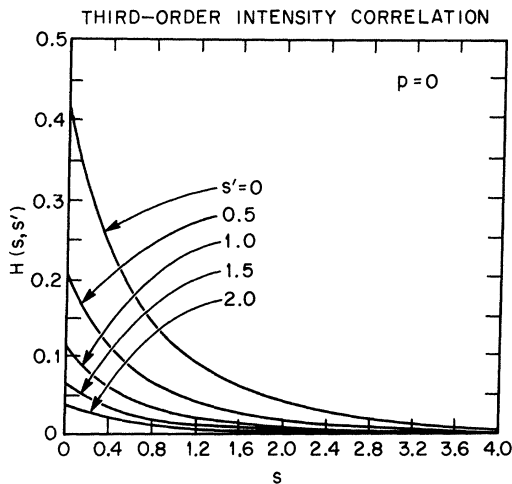


FIG. 2. Plot of $H(s, s')$ for $p = 0$, with units as described for Fig. 1.

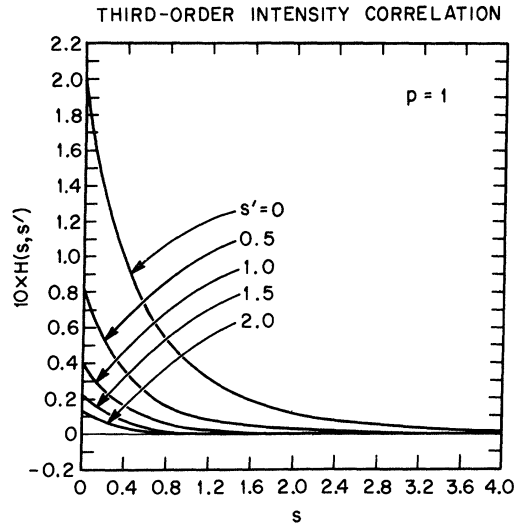


FIG. 3. Plot of $H(s, s')$ for $p = 1$, with units as described for Fig. 1.

depends on the normalized delay time s . For short delay times, the distribution is asymmetric towards positive fluctuations (as is always true below threshold); but for longer delay times the asymmetry favors negative fluctuations. If one can intuitively separate the appearance of a fluctuation from its subsequent decay, $\langle [\Delta\rho(0)]^2 \Delta\rho(s) \rangle$ can be viewed as an average of the value of a fluctuation s sec after it appears weighted with the square

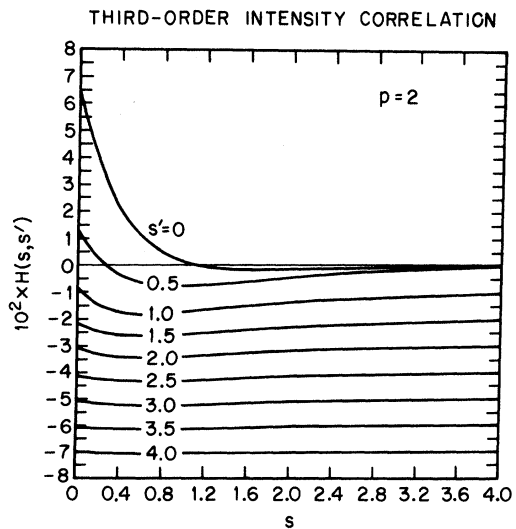


FIG. 4. Plot of $H(s, s')$ for $p = 2$, with units as described for Fig. 1. For clarity, the curves for $s' > 0.5$ have been displaced downwards successively by one unit per curve. In each case, the actual asymptote of $H(s, s')$ for large values of s is the s axis.

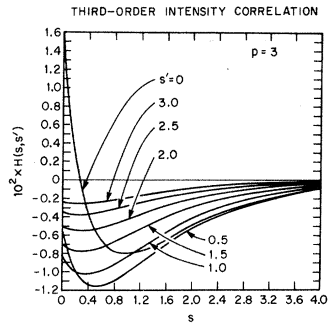


FIG. 5. Plot of $H(s, s')$ for $p=3$, with units as described for Fig. 1.

of its original magnitude. Thus, while fluctuations above the mean tend to be larger [$K_3(s, 0) > 0$ for $s=0$], they also decay more rapidly, leaving the negative fluctuations to predominate for longer delay times [$K_3(s, 0) < 0$ for s not near zero]. This behavior is physically reasonable, in view of saturation of the atomic population difference by the laser light. The same saturation effects which stabilize the intensity in a laser above threshold

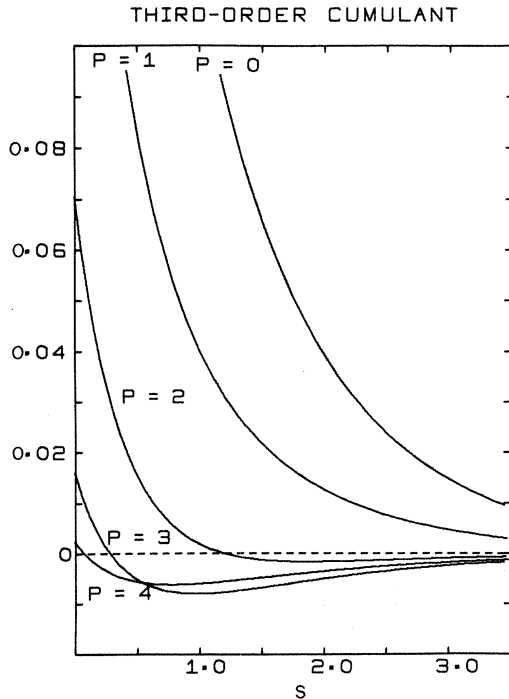


FIG. 6. Comparison plot of $H(s, 0)$ for several values of the pump parameter p in the threshold region. The oscillatory behavior of $H(s, 0)$ for $p > 1.5$ indicates a change in the asymmetry of the joint (two-time) intensity probability distribution. The units used are the same as in Fig. 1.

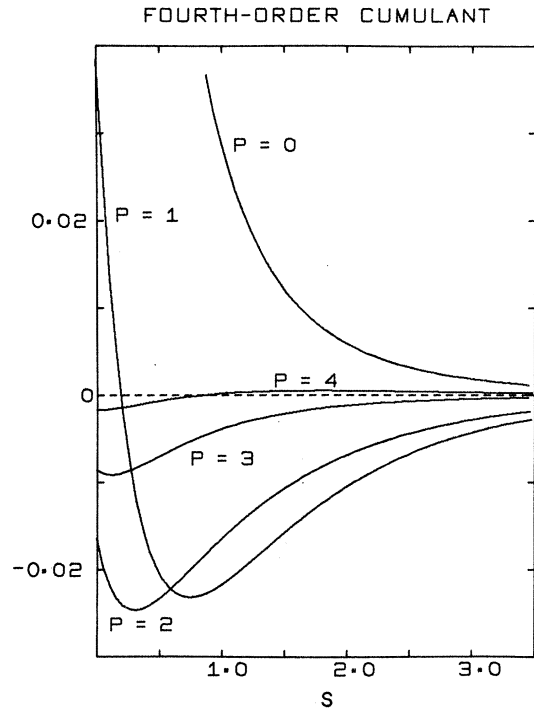


FIG. 7. Comparison plot of the normalized fourth-order intensity cumulant $K_4(s, 0, 0)$ [Eq. (18b)] as a function of normalized time delay s for several values of the pump parameter p in the threshold region. The units of time are the same as those used in Fig. 1. For each curve, K_4 is measured in units of \bar{p}^4 , where \bar{p} is the mean intensity of the laser at that value of p .

evidently damp the large intensity fluctuations above the mean more rapidly than those fluctuations below the mean.

Our results for the fourth- and fifth-order cumulants calculated from (18) are presented in Figs. 7 and 8. In the threshold region ($p = -1$ to $p = 2$) K_5 becomes negative for nonzero delay times, thus supporting the conclusions drawn from K_3 .

To present our results for H_3 in a compact form, we have fit a five-parameter expression of the form

$$H(s, s') = c_1 e^{-\lambda_1(s+s')/\bar{\Lambda}} + c_2 e^{-\lambda_2(s+s')/\bar{\Lambda}} + c_{12} (e^{-(\lambda_1 s + \lambda_2 s')/\bar{\Lambda}} + e^{-(\lambda_1 s' + \lambda_2 s)/\bar{\Lambda}}) \quad (25)$$

to our exact results for $H_3(s, s')$. The constants c_1 , c_2 , c_{12} , λ_1 , and λ_2 have been chosen so that the values of $H_3(0, 0)$, $[\partial H_3(s, 0)/\partial s]_{s=0}$, $\int_0^\infty H_3(s, 0) ds$, $\int_0^\infty s H_3(s, 0) ds$, and $\int_0^\infty H_3(s, s) ds$ are given exactly. While the form of (25) has no special significance, it is simple and gives a reasonably good fit to the values of $H_3(s, s')$ calculated from the more cumbersome expression (12). For the indicated values of p , Table I contains the constants

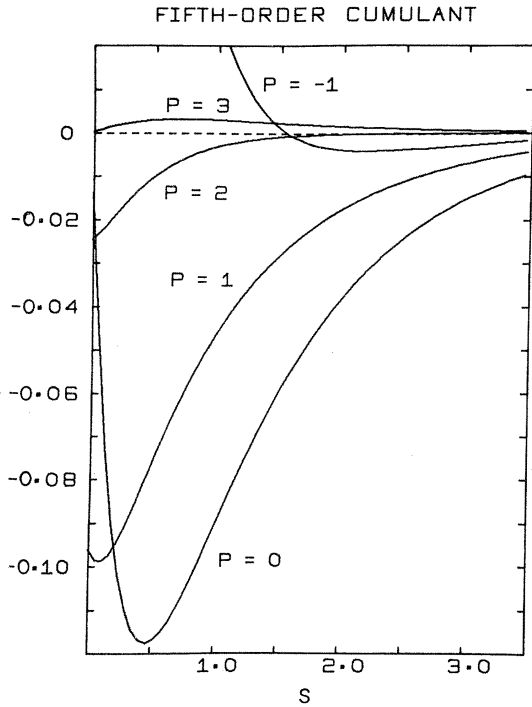


FIG. 8. Comparison plot of the normalized fifth-order intensity cumulant $K_5(s, 0, 0, 0)$ [Eq. (18c)] as a function of normalized time delay s for several values of the pump parameter p in the threshold region. The units of time are the same as those used in Fig. 1. For each curve, K_5 is measured in units of \bar{p}^{-5} , where \bar{p} is the mean intensity of the laser at that value of p .

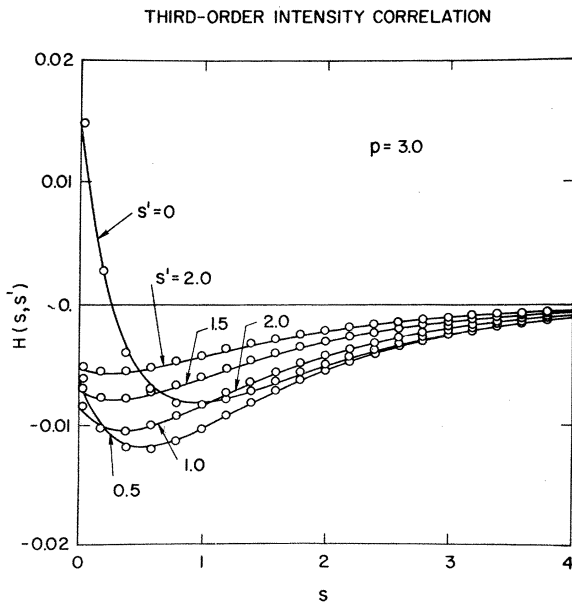


FIG. 9. Comparison plot of the exact third-order intensity cumulant $H(s, s')$ (smooth curves) and the approximate five-parameter fit [Eq. (25) and Table I (circles)].

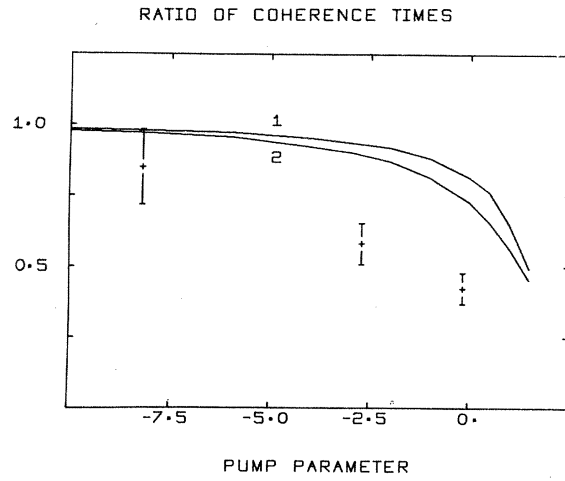


FIG. 10. Comparison between the calculated time required for $H(0, s)$ to decay to e^{-1} of its initial value (curve 1), one-half the time required to decay to e^{-2} of its initial value (curve 2), and the experimental results of Davidson and Mandel (Ref. 2). Far below threshold (p large and negative), curves 1 and 2 asymptotically approach 1.0, indicating that the second-order and third-order coherence times agree. Nearer threshold, the difference between curves 1 and 2 indicates the nonexponential time dependence of $H(0, s)$.

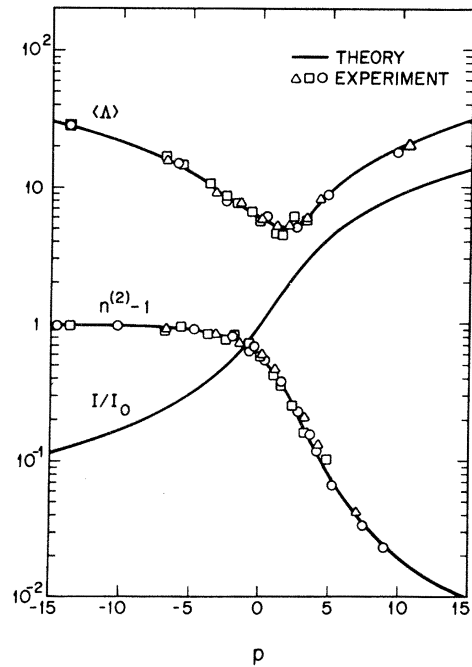


FIG. 11. Summary of experimental measurements of the reciprocal of the second-order coherence time $\langle \Lambda \rangle$, Eq. (22), and the second-order intensity cumulant at zero time delay, $n^{(2)} - 1$ [Eq. (15b), with $t=0$], as functions of the pump parameter p .

$c_1, c_2, c_{12}, \lambda_1,$ and λ_2 ; the reciprocal second-order coherence time $\bar{\Lambda}$; ΔH , the maximum difference between the exact $H_3(s, s')$ and (25); and $\Delta H/H_{\max}$, the ratio of ΔH to the maximum value of $|H_3(s, s')|$, expressed as a percent. Figure 9 contains a comparison plot of $H_3(s, s')$ and the five-parameter fit (25).

To compare our calculations to the experiments of Davidson and Mandel, we determined the experimental threshold intensity I_0 by fitting the measurements of $H_3(0, 0)$ versus intensity to the theoretical curves, thus finding the values of p corresponding to the measured intensities. For each value of the laser intensity, the experimental delay times at which the third-order cumulant was measured were divided by the measured second-order coherence time to obtain the normalized times s, s' . Davidson and Mandel report that $H_3(s, s')$ decays essentially exponentially to zero and can be characterized by a third-order coherence time. For the measured intensities (which were all below threshold) and the range of decrease of H_3 (roughly a factor of 5), the report of essentially exponential decay is consistent with these calculations. However, the measured third-order coherence times (shown in Fig. 10) are distinctly smaller than the calculated times which characterize the decay of H_3 . The

small amount of freedom in our determination of the time and intensity scales is inadequate to produce a substantially better agreement than is shown in Fig. 10. This situation contrasts sharply with the generally excellent agreement between experiment and the RWVP model for the mean reciprocal coherence time, the normalized second-order cumulant at zero time delay (Fig. 11), and the normalized higher-order cumulants at zero time delay (see Chang *et al.*⁴). These results suggest that more detailed measurements of the third-order intensity cumulant should be made, particularly above threshold, in order to look for the predicted oscillatory decay of $H_3(s, s')$ and provide more exacting test of the RWVP model.

ACKNOWLEDGMENTS

One of us (C.D.C.) wishes to thank Professor G. T. Reynolds of Princeton for his support of portions of this work, and the Aspen Center for Physics for its hospitality during preparation of an initial version of this paper. Another of us (W.A.S.) would like to thank B. A. Smith for her valuable assistance with the computer programming. We also thank Professor Frederic Davidson for useful conversations and B. C. Chambers for assistance in computer programming.

*Research at Princeton University was supported in part by the U. S. Atomic Energy Commission Division of Biology and Medicine under Contract No. AT(30-1)-3405, and by an institutional grant to Swarthmore College from the Alfred P. Sloan Foundation; research at City College was supported in part by A. R. O. D., O. N. R., and by a National Science Foundation Development Grant; research at New York University was supported in part by a National Science Foundation Institutional Grant.

†Part of this work was done while one of us (C. D. C.) was a Visiting Research Fellow in the Department of Physics, Princeton University.

¹Some of the results reported in this paper were reported earlier by C. D. Cantrell and W. A. Smith [Phys. Letters **37A**, 167 (1971)]; M. Lax arrived at the same results independently. We have decided to publish them together.

²F. Davidson and J. Mandel, Phys. Letters **25A**, 700 (1967); more details are contained in F. Davidson, Phys. Rev. **185**, 446 (1969).

³F. Haake, Z. Physik **227**, 179 (1969); Phys. Rev. A **3**, 1723 (1971).

⁴A statistician's formulation of cumulants is contained in M. G. Kendall and A. Stuart, *The Advanced Theory of Statistics* (Hafner, New York, 1958), Vol. I, Chap. 3.

A general formulation for many times and for noncommuting operators was given by R. Kubo [J. Phys. Soc. Japan **17**, 1100 (1962)]. The use of cumulants in quantum optics has been emphasized by R. F. Chang, V. Korenman, C. O. Alley, and R. W. Detenbeck [Phys. Rev. **178**, 612 (1969)] and C. D. Cantrell [Phys. Rev. A **1**, 672 (1970)].

⁵M. Lax, Phys. Rev. **172**, 350 (1968).

⁶H. Haken and W. Weidlich, Z. Physik **205**, 96 (1967).

⁷The Markoffian property was not used in Ref. 5 in setting up the multitime correspondence, but only in factoring the resulting probability distributions.

⁸M. Lax, in *Statistical Physics, Phase Transitions, and Superfluidity*, edited by M. Chrétien, E. P. Gross, and S. Deser (Gordon and Breach, New York, 1968), Vol. 2.

⁹P. M. Morse and H. Feshbach, *Methods of Theoretical Physics* (McGraw-Hill, New York, 1953), pp. 884-886.

¹⁰M. Lax and M. Zwanziger, Phys. Rev. A (to be published).

¹¹H. Risken and H. D. Vollmer, Z. Physik **201**, 323 (1967).

¹²R. D. Hempstead and M. Lax, Phys. Rev. **161**, 350 (1967).

¹³C. D. Cantrell and W. A. Smith (unpublished).